STEM CELLS AND DEVELOPMENT
Volume 23, Number 24, 2014

DOI: 10.1089/scd.2013.0560

CXCL12/Stromal-Cell-Derived Factor-1 Effectively Replaces Endothelial Progenitor Cells to Induce Vascularized Ectopic Bone

Rhandy M. Eman,[1] Edgar T. Hoorntje,[1] F. Cumhur Öner,[1] Moyo C. Kruyt,[1] Wouter J.A. Dhert,[1,2] and Jacqueline Alblas[1]

Bone defect healing is highly dependent on the simultaneous stimulation of osteogenesis and vascularization. In bone regenerative strategies, combined seeding of multipotent stromal cells (MSCs) and endothelial progenitor cells (EPCs) proves their mutual stimulatory effects. Here, we investigated whether stromal-cell-derived factor-1α (SDF-1α) stimulates vascularization by EPCs and whether SDF-1α could replace seeded cells in ectopic bone formation. Late EPCs of goat origin were characterized for their endothelial phenotype and showed to be responsive to SDF-1α in in vitro migration assays. Subsequently, subcutaneous implantation of Matrigel plugs that contained both EPCs and SDF-1α showed more tubule formation than constructs containing either EPCs or SDF-1α. Addition of either EPCs or SDF-1α to MSC-based constructs showed even more elaborate vascular networks after 1 week in vivo, with SDF-1α/MSC-laden groups showing more prominent interconnected networks than EPC/MSC-laden groups. The presence of abundant mouse-specific CD31/PECAM expression in these constructs confirmed ingrowth of murine vessels and discriminated between angiogenesis and vessel networks formed by seeded goat cells. Importantly, implantation of EPC/MSC or SDF-1α/MSC constructs resulted in indistinguishable ectopic bone formation. In both groups, bone onset was apparent at week 3 of implantation. Taken together, we demonstrated that SDF-1α stimulated the migration of EPCs in vitro and vascularization in vivo. Further, SDF-1α addition was as effective as EPCs in inducing the formation of vascularized ectopic bone based on MSC-seeded constructs, suggesting a cell-replacement role for SDF-1α. These results hold promise for the design of larger centimeter-scale, cell-free vascular bone grafts.

Introduction

A poor vascular network in and around larger bone grafts often impairs the healing of bone [1,2]. Inappropriate vascularity leads to compromised survival of recruited and/or seeded cells in the grafts, as nutrient and oxygen supply is limited [3]. In addition, inadequate vascularity may have indirect negative effects on other risk factors that play a role during bone healing, such as the production, release, and/or effectivity of growth factors that are produced during fracture [2]. Therefore, the past years studies have focused on tissue-engineered grafts that promote vascularization [4–6]. One of the strategies investigated includes the seeding of constructs with endothelial progenitor cells (EPCs) [6]. It has been proven that the use of endothelial cells (ECs) or their progenitors (EPCs) improves vascularization by inducing the formation of blood vessel networks that connect to the host circulation [7]. Moreover, when ECs are combined with multipotent stromal cells (MSCs), communication between both cell types positively influences osteogenic differentiation in vitro [7–11] as well as bone formation in vivo [5–8]. To this end, an optimal ratio of both cell types leads to higher efficiency in the formation of tubular structures [7,9,12,13] and mineralization [7,9,10] in vitro, when compared with single-cell-type cultures. When implanted in vivo, ectopic implantations show that combined constructs contain higher density of vasculature than the seeding of MSCs alone [9,12,14] and that bone formation is positively affected by the addition of ECs or EPCs [8–10]. At orthotopic locations, some studies claim that there is no beneficial effect on total vessel formation after implantation [6,15], while other results show significantly higher early vascularization using EPCs in combination with MSCs [5,6]. In addition, the stimulating effect on bone formation using combinations of MSCs and ECs or EPCs varies between studies [5,6,15].

[1]Department of Orthopedics, University Medical Center Utrecht, Utrecht, The Netherlands.
[2]Faculty of Veterinary Medicine, Utrecht University, Utrecht, The Netherlands.

Another strategy to improve vascularization of implants is the inclusion of growth factors that promote angiogenesis, such as vascular endothelial growth factor [16–19] and C-X-C motif ligand 12/stromal cell-derived factor-1α (CXCL12/SDF-1α) [20–22]. SDF-1α is known to be active as a potent cell-homing factor [23–25] through binding to its CXCR4 receptor [26] and has been proven to induce tubule formation by ECs in vitro [20,21] as well as angiogenesis in tissue-engineered grafts in vivo [20,23,27]. However, its role in the formation of vascularized bone has not been investigated yet, contrary to the use of growth factors that promote osteogenesis in bone grafts [18,28–30]. Moreover, studies that investigate replacement of cell seeding by growth factors in order to optimize the use of cell-free applications that promote vascularized bone formation are lacking, while it is highly desirable to overcome the disadvantages of cell isolation and extensive cell culture [31]. Therefore, we investigated the use of EPCs and MSCs and the chemokine SDF-1α, in combination or as single applications, in ectopic hybrid constructs to induce vessel formation and subsequent bone formation. We hypothesized that SDF-1α stimulates vessel formation by seeded EPCs in ectopic bone grafts and hereby may affect the onset of bone formation and as a result bone volume. In addition, based on previous experiments [7] we investigated whether SDF-1α can effectively replace EPCs in MSC-based bone-forming constructs.

Materials and Methods

Cell culture

Cells of goat origin were obtained from previous experiments [7] and used in view of future translation toward implantations in the goat model [31,32]. To this end, MSCs were isolated from the iliac crest bone marrow of adult Dutch milk goats as previously described [32]. In short, the bone marrow aspirate was plated in alpha-minimum essential medium (α-MEM) supplemented with 10% (v/v) fetal calf serum, 100 U/mL penicillin, 100 μg/mL streptomycin, and 0.2 mM L-ascorbic acid-2-phosphate (AsAP) and multipotency was tested using established protocols [33]. Passage 2–4 cells were used for all experiments.

EPCs were isolated from peripheral blood samples from adult Dutch milk goats as previously described [7]. Briefly, MNCs were isolated by Ficoll density gradient centrifugation and cells were plated in fibronectin-coated flasks in complete EBM-2 medium (Lonza) with 20% (v/v) fetal calf serum. Passage 10–13 cells were used in all experiments.

Characterization of late EPCs

To analyze the uptake of DiI-labeled, acetylated low-density lipoprotein (LDL) complex and isolectin B_4 by cultured EPCs, cells were cultured on cover slips until confluent and subsequently incubated for 1 h with fluorescein-labeled isolectin B_4 (Vector Laboratories) followed by 2-h incubation with DiI-labeled, acetylated LDL complex (Molecular Probes, Invitrogen) at 37°C. Thereafter, the cells were washed with PBS and mounted in Vectashield including DAPI (Vector Laboratories). Cells were analyzed for double positivity.

For the analysis of CD31/PECAM-1 expression on ECs, trypsinized cells were kept in suspension overnight, washed with PBS, and incubated with mouse anti-ovine CD31 (100 μg/mL; Serotec) for 1 h at 4°C and subsequently with Alexa Fluor 488 goat anti-mouse IgG (20 μg/mL in PBS; Invitrogen) at 4°C for 45 min. Cells were analyzed by FACS (FACS Calibur; Becton Dickinson) and CELLQuest software (Becton Dickinson).

To assess network formation by cultured EPCs, angiogenesis assays were performed [In Vitro Angiogenesis Assay Kit (Chemicon)], according to manufacturer's instructions. About 10^4 EPCs were seeded on top of Matrigel discs and incubated in complete EBM-2 medium and 20% (v/v) fetal calf serum for 22 h and then imaged.

In vitro transwell migration assay

To evaluate the responsiveness of goat EPCs to rhSDF-1α (R&D Systems), transwell migration assays were performed (24 wells, 8-μm pore; Corning Costar). Upper wells were seeded with 10^5 EPCs. Lower chambers were supplemented with 500-μL medium containing 0, 10, 50, or 100 ng/mL SDF-1α. Experiments were carried out in duplicate for 18 h, whereafter the migrated cells on the bottom side of the membranes were counted in four randomly chosen fields. Experiments were repeated twice.

Preparation of in vivo implants

To evaluate the effect of single applications or combinations of rhSDF-1α, EPCs, and/or MSCs on vessel formation (week 1) and bone formation (week 6), 200 μL of growth-factor-reduced Matrigel (BD Biosciences) constructs was prepared for subcutaneous implantation in nude mice ($n = 23$). Plugs consisted of (1) SDF-1α, (2) EPCs, (3) SDF-1α/EPCs, (4) EPCs/MSCs, and (5) SDF-1α/MSCs. Groups 2 and 4 contained a total of 2.5×10^5 cells per construct; group 3 and 5 contained 1.25×10^5 cells. Matrigel plugs were supplemented with 1 μg/mL rhSDF-1α where indicated. In addition, all constructs contained 20% (w/v) of BCP particles (0.5–1 mm Ø, BCP-1150; Xpand).

Animals and implantation

Twenty-three female nude mice (Hsd-cpb:NMRI-nu; Harlan) were anesthetized with 2.0%–2.5% isoflurane, after which the implants were placed in five separate subcutaneous pockets, using a randomized design. The animals were postoperatively treated with the analgesic buprenorphine (0.05 mg/kg, sc; Temgesic, Schering-Plough/Merck) and housed together at the Central Laboratory Animal Institute, Utrecht University. Six mice received fluorochrome labels at week 3 (Calcein green, 3 mg/mL s.c.; Sigma), week 4 (Oxytetracyclin, 2 mg/L s.c.; Calbiochem), and week 5 (Xylenol Orange, 20 mg/mL s.c.; Sigma) to determine the onset of bone formation. Experiments were conducted with the permission of the local Ethical Committee for Animal Experimentation and in compliance with the Institutional Guidelines on the use of laboratory animals.

Explantation and embedding

One of the mice died unexpectedly during the operation. After 1 week ($n = 16$) and 6 weeks ($n = 6$), constructs were retrieved and fixed overnight in 4% (v/v) formalin and

processed for 5-μm-thick paraffin sections through alcohol dehydration series. In addition, half of all week-6 samples were processed for polymethylmethacrylate (MMA; Sigma) embedding and sectioned to analyze bone formation and fluorochrome deposition.

Evaluation of the formation of vessel networks

Vessel network formation in the constructs after 1 week of implantation was evaluated using Goldner's trichrome staining on rehydrated sections and was based on established protocol [34]. Samples were blinded and formed network structures were scored by two observers as follows: Grade 1, single cells and/or the presence of microluminal structures; Grade 2, luminal-vessel-like structures of which some were erythrocyte perfused; or Grade 3, interconnected networks, some perfused with erythrocytes. Three randomly chosen fields per construct were analyzed for the mean length of formed tubule complexes, referred to as an average of the actual total lengths of formed tubule complexes within several views. In addition, the number of formed junctions was quantified. For both parameters, Angioquant [35] was used.

Immunohistochemistry of CD31/PECAM-1

Vessels formed in the constructs were stained for mouse-specific CD31/PECAM-1 expression. Antigen retrieval was performed on rehydrated sections by incubation in 0.1 M sodium citrate solution (pH = 6.0) for 20 min at 95°C. Sections were then blocked in 3% (v/v) H_2O_2 in PBS for 15 min and 5% (w/v) BSA for 1 h at room temperature. Primary rabbit anti-CD31 (LifeSpan Biosciences) was incubated at 2 μg/mL overnight at 4°C. A secondary goat anti-rabbit biotinylated antibody (0.6 μg/mL; DakoCytomation) and streptavidin-peroxidase (1.4 μg/mL; DakoCytomation) were incubated each for 30 min at room temperature. The staining was developed with diaminobenzidine and Mayer's hematoxylin was used for counterstaining. Negative controls were treated similarly, except for exclusion of the primary antibody. As a positive control for antibody specificity, mouse skin was included.

Histomorphometry and fluorochrome analysis

Of the MMA-embedded samples, 10-μm sections were cut (Leica) and evaluated for the deposition of the different fluorochromes that were incorporated into the newly formed bone. Visualization of the fluorochromes was performed using a light/fluorescence microscope (E600; Nikon), equipped with a quadruple filter block (XF57, dichroic mirror 400, 485, 558, and 640 nm; Omega Optics). Three sections per construct were scored for the presence of the three different fluorochromes. All of the week-6 constructs were evaluated. Thereafter, the sections were stained by basic fuchsin/methylene blue to evaluate bone formation using a light microscope. Bone and scaffold were pseudo-colored and histomorphometry was performed using a custom macro of the KS400 software (version 3; Zeiss) to determine the scaffold outline available for bone apposition and the contact length of bone and scaffold. Bone area % was calculated as [bone area/(total area – BCP scaffold area)] $\times 100\%$. Bone contact % was calculated as (bone-to-scaffold contact length/scaffold outline) $\times 100\%$.

Statistical analysis

Statistical analysis was performed with SPSS 20.0 software. A Mann–Whitney U test was used to compare the number of migrated cells in the transwell assays. The evaluation of the formation of vessel networks (Fig. 4) was subjected to a Chi-square test and Bonferroni corrections were applied to calculate statistical differences between the groups. The mean length of formed tubule complexes, the number of junctions, and bone area and contact percentages were tested by a randomized one-way ANOVA with Bonferroni correction. $P < 0.05$ was considered statistically significant.

Results

In vitro stimulation of goat EPC migration by SDF-1α

Isolated goat EPCs were characterized for their endothelial phenotype by selected markers. Cells were double positive for the uptake of DiI-labeled, acetylated LDL complex and isolectin B_4 (Fig. 1A). In addition, the late endothelial marker CD31/PECAM1 was expressed at this passage on the cells, as shown by FACS analysis (Fig. 1B). When the cells were seeded on Matrigel for the angiogenesis assay, they formed interconnected networks (Fig. 1C), indicating their tubule-forming phenotype. Since SDF-1α is a known chemoattractant for various cell types, we assessed its function in the in vitro stimulation of goat EPC migration. Seeded EPCs appeared highly responsive to rhSDF-1α, showing a significant 2- to 2.5-fold increase in migration capacity at increasing concentrations of the chemokine (Fig. 2).

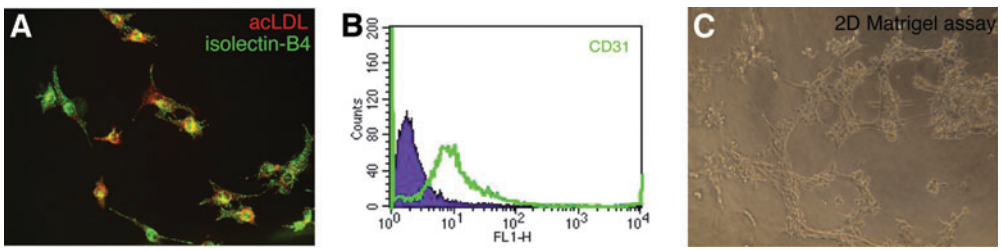

FIG. 1. Characterization of goat late endothelial progenitor cells (EPCs). Isolated goat late EPCs were characterized by the uptake of DiI-labeled, acetylated low-density lipoprotein (LDL) complex (*red*) and isolectin B_4 (*green*) **(A)**. The presence of the selected endothelial marker CD31/PECAM was shown by FACS analysis in *green* **(B)** against the negative control in *purple*. The isolated cells showed their endothelial phenotype by the formation of tubules in a 2D angiogenesis assay **(C)**. Color images available online at www.liebertpub.com/scd

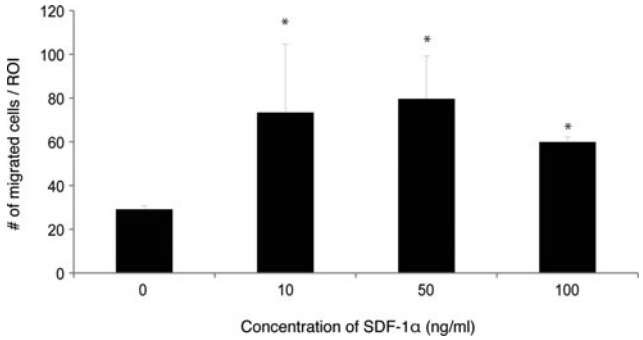

FIG. 2. In vitro transwell migration assay. Significantly (*$P < 0.05$) higher numbers of EPCs migrated toward rhSDF-1α at 10, 50, or 100 ng/mL when compared with negative controls. Migration is expressed as mean ± SD.

In vivo vessel network formation

After 1 week of implantation, Grade 1 structures were observed in constructs containing SDF-1α (Fig. 3A) or seeded EPCs (Fig. 3B). When combining seeded EPCs with SDF-1α, both Grade 1 and Grade 2 structures were observed (Fig. 3C), of which perfusion of Grade 2 luminal-vessel-like structures with erythrocytes was observed. Grade 2 morphologies were found in a slightly higher percentage of SDF-1α/EPC constructs than in constructs of either type alone (Fig. 4), showing the beneficial effect of SDF-1α on EPCs. In EPC/MSC constructs we found predominantly the formation of Grade 2 structures (Figs. 3D and 4), some of which were erythrocyte perfused, demonstrating their connection to the host circulation. In addition, 36% of the EPC/MSC constructs showed elaborate interconnected network (Grade 3) structures. Of great interest are the combined SDF-1α/MSC constructs, where the majority, namely, 69%, of the constructs showed abundant Grade 3 structures (Figs. 3E and 4). Also, similar to SDF-1α/EPC and EPC/MSC constructs, perfusion of the interconnected networks could be observed by the presence of erythrocytes. In addition, the expression of the mouse-specific endothelial CD31/PECAM marker in the combination groups confirmed the contribution of the host cells and SDF-1α to angiogenesis. Vessel network formation by the seeded goat cells could be concluded from vessels that were negative for CD31/PECAM

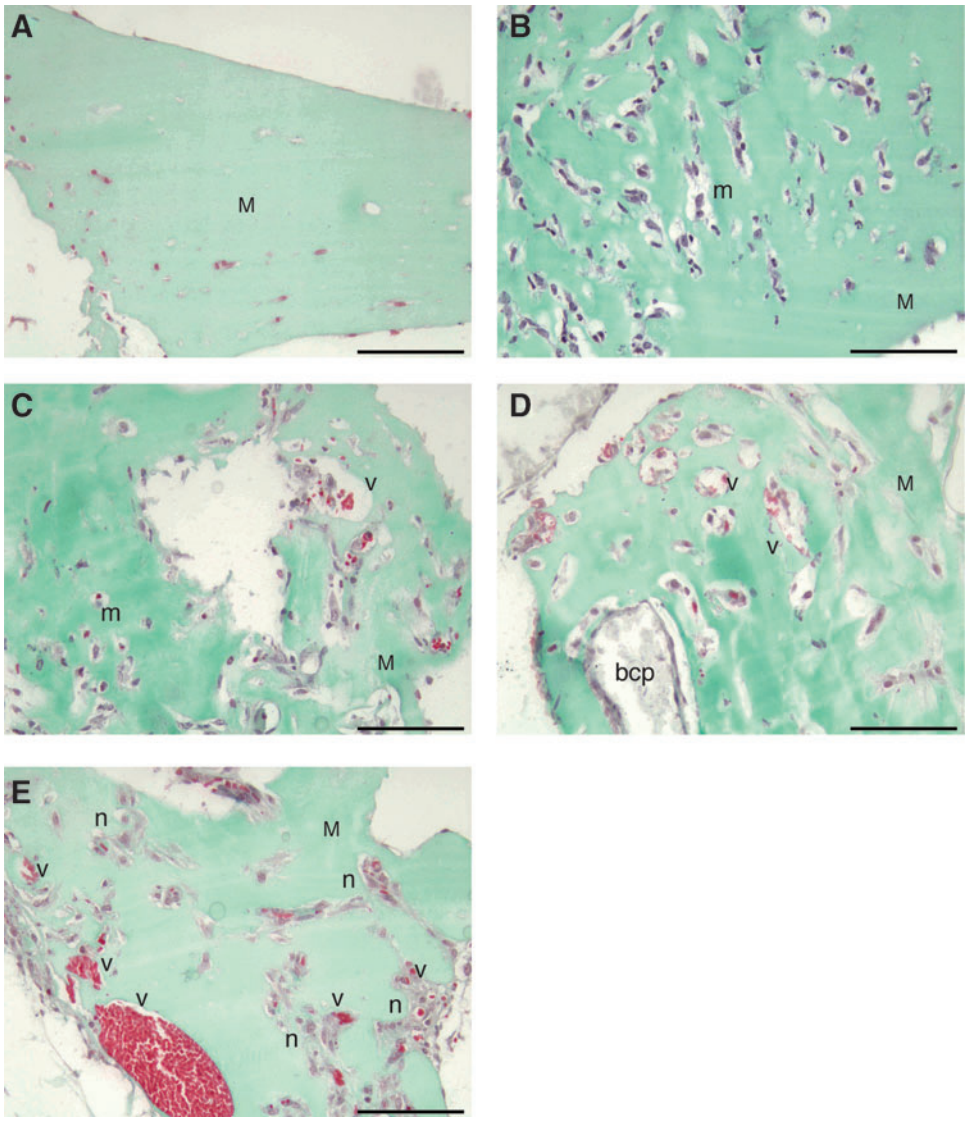

FIG. 3. Evaluation of vessel network formation after 1 week of implantation. Goldner's-trichrome-stained sections showed the presence of single cells and/or the formation of microluminal structures (m) in stromal-cell-derived factor-1α (SDF-1α) constructs **(A)** or constructs containing seeded late EPCs **(B)** after 1 week of implantation. SDF-1α/EPC containing constructs **(C)** showed more luminal-vessel-like structures (v). EPC/multipotent stromal cell (MSC) constructs **(D)** showed predominantly luminal-vessel-like structures, as well as elaborate interconnected networks (n). When combining SDF-1α with MSCs **(E)**, mainly elaborate interconnected networks were observed (n). M, Matrigel; bcp, biphasic calcium phosphate; m, microluminal structures; v, luminal-vessel-like structures; n, elaborate interconnected networks. Scale bars represent 100 μm. Color images available online at www.liebertpub.com/scd

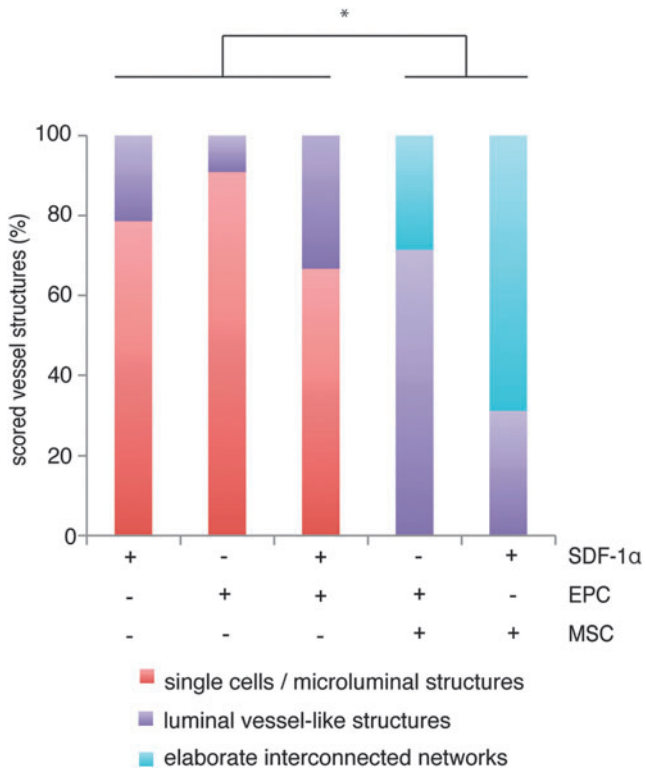

FIG. 4. Scoring of vessel network formation in the implanted constructs after 1 week of implantation. Scoring of the morphology of vessel network formation was done on Goldner's-trichrome-stained sections and could be subdivided as follows: Grade 1, single cells and/or the presence of microluminal structures; Grade 2, luminal-vessel-like structures; or Grade 3, elaborate interconnected networks. +/ − indicates inclusion of SDF-1α, EPCs, or MSCs in the hybrid constructs. EPC/MSC and SDF-1α/MSC groups showed significantly (*$P < 0.05$) different vessel network formation efficiency than SDF-1α, EPC, and SDF-1α/EPC groups. Color images available online at www.liebertpub.com/scd

(Fig. 5A–C), as all vessels in the host mouse skin were positive for CD31/PECAM (Fig. 5D). Both phenotypes were observed in SDF-1α/EPC, EPC/MSC, and SDF-1α/MSC groups.

Quantification of formed vessel networks

To evaluate the characteristics of the formed networks in all constructs, the mean length of the formed tubule complexes and the number of formed junctions in the five different groups were quantified. More Grade 2 luminal-vessel-like structures were observed in SDF-1α/EPC constructs when compared with either type alone, but no significant differences were found in the mean length of the formed tubule complexes or the number of formed junctions between SDF-1α/EPC groups and constructs containing either factor alone (group 3 vs. groups 1 and 2; Fig. 6A, B). As expected, both the mean length of the formed tubule complexes as well as the number of formed junctions in the MSC-based groups were significantly higher than constructs containing either EPCs or SDF-1α (groups 4 and 5 vs. groups 1 and 2; Fig. 6A, B). When comparisons were made between the combination constructs (groups 3, 4, and 5), the mean length of the formed tubule complexes was significantly lower in SDF-1α/EPC constructs when compared with SDF-1α/MSC groups (Fig. 6A), suggesting different effects of SDF-1α on vascularization induced by EPCs and MSCs. The number of formed junctions was significantly higher in both MSC-based constructs (groups 4 and 5) when compared with SDF-1α/EPCs (group 3; Fig. 6B). In addition, no significant differences were found in the mean length of the formed tubule complexes (Fig. 6A) or in the number of formed junctions (Fig. 6B) when EPC/MSC constructs (group 4) were compared with SDF-1α/MSC constructs (group 5), suggesting that SDF-1α efficiently replaces EPC seeding in MSC-based constructs to stimulate early blood vessel formation.

Bone formation and the onset of bone formation

To investigate the possibility of SDF-1α as a replacement for cell seeding in the bone formation process, bone onset, bone volume percentages, and bone contact percentages were measured. Constructs containing EPCs/MSCs or SDF-1α/MSCs started to form bone at 3 weeks and this continued at least until week 5 as all three fluorochromes were present in all of the scored sections (Fig. 7A, B). No differences in bone onset between the two constructs could be observed. Bone that was formed (Fig. 7C, D) showed similar mean bone volumes in EPC/MSC-loaded constructs when compared with SDF-1α/MSC-loaded constructs (Fig. 7E), suggesting an EPC-seeding-replacement role for SDF-1α in the enhancement of ectopic bone formation. Also, mean bone contact percentages between the two MSC-based groups showed no significant differences (Fig. 7E). Groups that contained SDF-1α, EPCs, or SDF-1α/EPCs did not show any deposition of fluorochromes as no bone formation was observed (data not shown). These findings strongly suggest that the need for an osteogenic stimulus in the form of MSCs is higher than the need for seeded EPCs to form vascularized ectopic bone in vivo.

Discussion

In this study, we showed the effectiveness of the chemokine SDF-1α as a stimulator of early blood vessel formation by seeded cells in ectopic constructs in vivo. More importantly, we showed that SDF-1α could be used as a replacement for EPC-seeding strategies in bone-forming constructs, without affecting bone volumes or bone contact percentages.

The effectiveness of human recombinant SDF-1α on isolated goat EPCs in terms of migration in vitro was shown, which confirms that cells of goat origin can be stimulated by the chemokine of human origin. In vitro migration of EPCs using concentrations of 50 ng/mL SDF-1α or lower has been shown before with human cells [20,21]. However, this phenomenon has not been evaluated previously for cells of goat origin and broadens our future use of both factors in the optimization of hybrid constructs containing cells of goat origin and/or SDF-1α. Subsequently, when implanted in subcutaneous pockets, constructs containing single applications of SDF-1α or EPCs showed the presence of single cells and/or microluminal structures after 1 week of implantation,

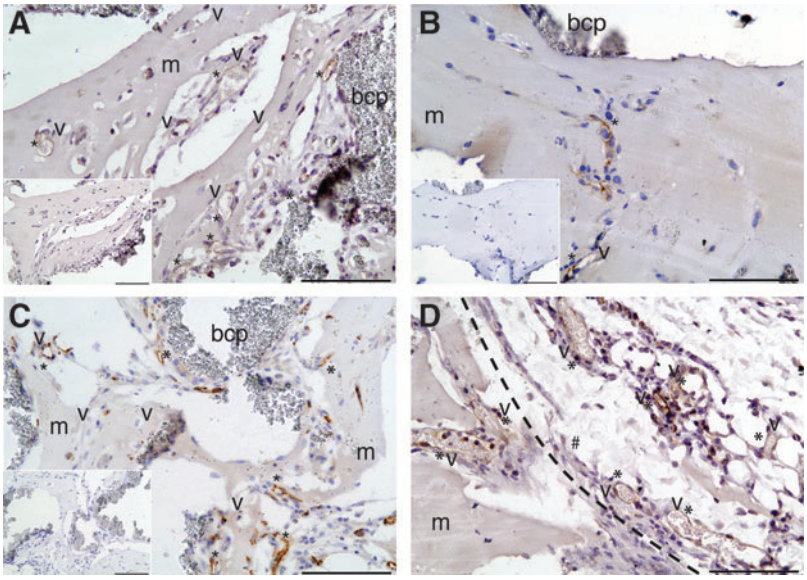

FIG. 5. Evaluation of the endothelial identity of formed vessel structures. In the three combination constructs—SDF-1α/EPC **(A)**, EPC/MSC **(B)**, and SDF-1α/MSC **(C)**—abundant expression of the mouse-specific CD31/PECAM-1 marker was found on the vessels. As a positive control, all vessels in the host mouse skin (#), separated by the *dashed line*, were positive for CD31/PECAM **(D)**. Representative negative control stainings for all combined constructs are shown by the *insets*. M, Matrigel; bcp, biphasic calcium phosphate; V, vessel; *positive CD31/PECAM staining; #host mouse skin. Scale bars represent 100 μm. Color images available online at www.liebertpub.com/scd

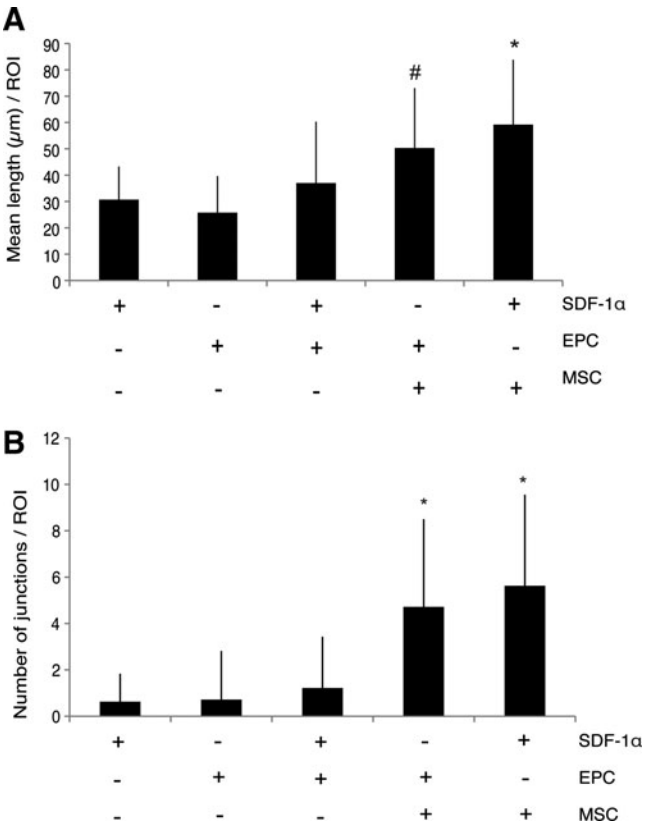

FIG. 6. Quantification of the formed vessel structures after 1 week in vivo. The mean length of formed tubule complexes **(A)** was significantly different between constructs containing SDF-1α or EPCs when compared with EPC/MSC constructs ($^{\#}P < 0.05$). SDF-1α/MSC constructs showed significantly longer tubule complexes when compared with SDF-1α, EPC, or SDF-1α/EPC constructs ($^{*}P < 0.05$). The numbers of formed junctions **(B)** in the constructs were significantly higher in EPC/MSC or SDF-1α/MSC constructs when compared with SDF-1α, EPC, or SDF-1α/EPC constructs ($^{*}P < 0.05$). Data are expressed as mean ± SD.

suggesting ongoing vascularization. This is in accordance to other studies [12,14,23,36]. Hybrid constructs containing both SDF-1α and EPCs showed a slightly higher percentage of luminal-vessel-like structures than either type alone. This phenomenon supports the observed in vitro stimulating effect of SDF-1α on network formation by EPCs by others. When discriminating between angiogenesis and the luminal-vessel-like structures formed by the seeded EPCs, we found mainly perfused vessels that were positive for the mouse-specific CD31/PECAM-1 antibody. This points to induction of host angiogenesis in these constructs as a result of combined cell/chemokine therapy. In addition, throughout the constructs we also found luminal-vessel-like structures, which were likely formed by the goat EPCs as a result of SDF-1α stimulation, since constructs containing only EPCs hardly showed this phenomenon. To our knowledge, we are the first to report these findings by using combined cell/chemokine therapy in vivo.

The past years, several studies in the field of tissue engineering have focused on combined cell treatment to induce vascularization [6,7,14,37,38]. When we combined EPCs and MSCs in our hybrid constructs, we observed more luminal-vessel-like structures as well as elaborate interconnected vessel networks when compared with constructs containing the single growth factor SDF-1α, EPCs alone, or the combination of SDF-1α and EPCs. This is in accordance to our previous experiments [7] and other reports [9,12,14]. In addition, the formed vessel networks had a significantly higher mean length when compared with the single EPC or SDF-1α constructs. The number of formed junctions was significantly higher when compared with SDF-1α, EPC, or SDF-1α/EPC constructs, supporting the observed interconnection of the formed vessel networks. In EPC/MSC constructs, both angiogenesis and vasculogenesis could be observed by means of CD31/PECAM-1 staining. This is in accordance to a study by Liu et al. [9], in which they showed that combined seeding of EPCs and MSCs resulted in a higher degree of host-derived neovascularization than vessel formation by seeded cells. Others report the contrary [14,39], although this may be explained by the different

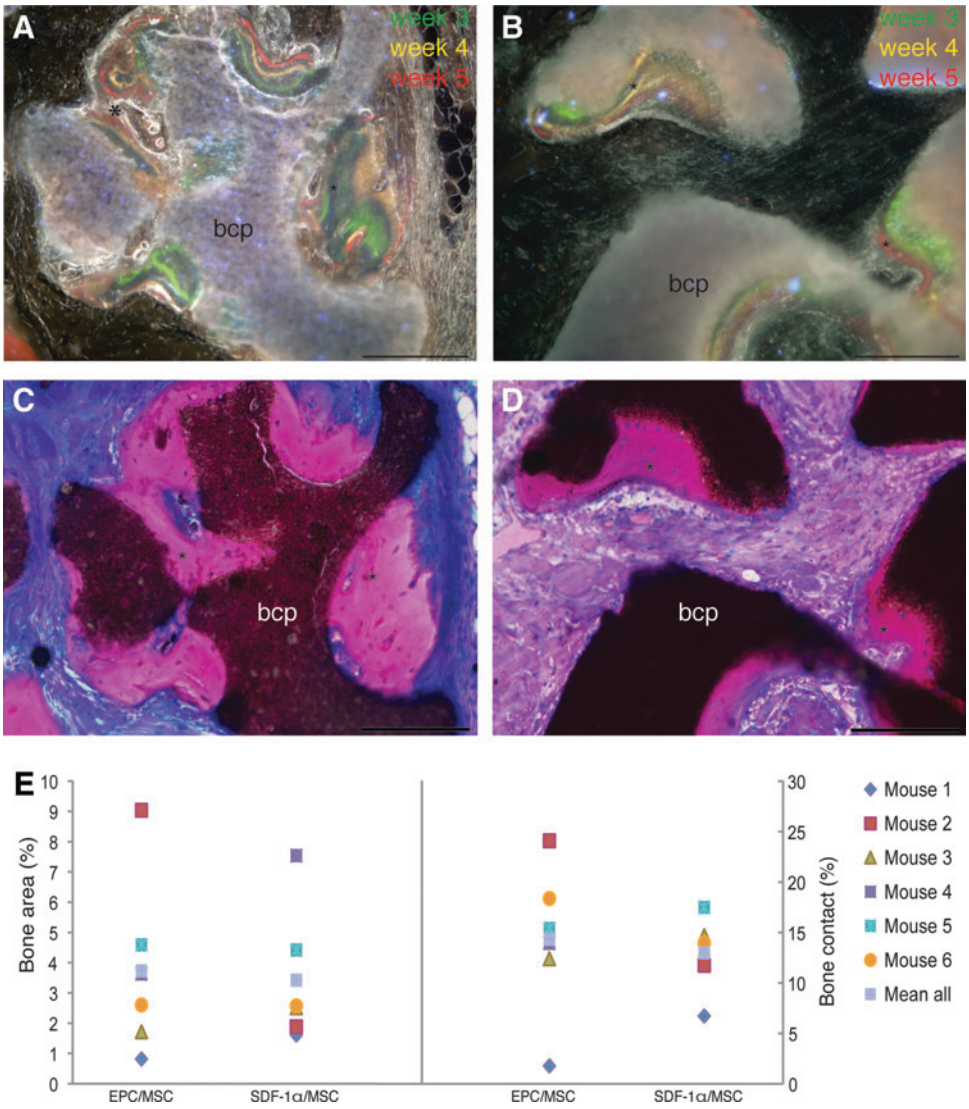

FIG. 7. Evaluation of bone formation after 6 weeks of implantation. Unstained MMA-embedded sections showed the presence of the fluorochromes calcein green (week 3; *green*), oxytetracyclin (week 4; *yellow*), and xylenol orange (week 5; *red*). Bone formation started before week 3 for both EPC/MSC **(A)** and SDF-1α/MSC **(B)** constructs. Basic fuchsin/methylene *blue* staining revealed bone formation in *pink* in EPC/MSC **(C)** and SDF-1α/MSC **(D)** constructs, with no significant differences between the two groups in either bone volume % or bone contact % **(E)**. bcp, biphasic calcium phosphate; * bone. Scale bars represent 200 μm. Color images available online at www.liebertpub.com/scd

source of the used cells [40] as well as the period the cells have been in culture.

Most importantly, combining SDF-1α with MSCs resulted in the highest degree of interconnected vessel networks when compared with all other four groups. Moreover, the mean length of the formed tubule complexes and the number of junctions were not significantly different from EPC/MSC constructs. These results indicate a preference for SDF-1α as a stimulator of vascularization in the MSC-based constructs rather than the use of EPCs. The formed tubular networks in SDF-1α/MSC constructs were clearly anastomosed microvessels, as shown both by the extensive CD31/PECAM-1 positivity in the constructs as well as the perfusion of the networks with blood. These results suggest not only induction of angiogenesis and/or recruitment of host ECs, as confirmed by positive mouse-specific endothelial staining, but also the possible transition of MSCs toward the endothelial lineage as CD31/PECAM-1 negativity was also observed in most of the elaborate vessel networks, a phenomenon also described by others [41,42]. However, the presence of some early EPCs in the MSC fraction is also possible, although these cells are found at low frequencies in MSC isolates. Unfortunately, at present a goat-specific endothelial antibody is not available, thus excluding further identification of these cells.

The additive effect of EPCs on MSCs in bone formation, as well as in vasculogenesis, has been described previously by us and others [7,9,12,14]. As this study focused mainly on the possible replacement of seeded cells by SDF-1, which was based on previous experiments by our group [7], we did not include a group containing only MSCs. Moreover, we have recently confirmed this knowledge in a different study that applies various EPC subtypes and show here the additive effect of EPCs on both vessel formation and bone formation subcutaneously in vivo when compared with MSCs alone (Eman et al., article in preparation). Here, we investigated the possible replacement of EPCs by SDF-1α in ectopic hybrid bone constructs, and showed the induction of comparable bone onset, bone volumes, and bone contact percentages between EPC/MSC and SDF-1α/MSC groups, while SDF-1α/MSC groups showed the highest degree of interconnected vessel networks. This finding supports the replacing role of EPCs by SDF-1α to form vascularized ectopic bone in constructs containing osteoprogenitors in the

form of MSCs. It would be interesting to investigate this application in larger centimeter-scale bone replacement constructs, where vasculogenesis is likely the limiting factor for bone formation. Until now, there are no strong indications that SDF-1α could recruit enough cells to fully replace MSC seeding in a mouse subcutaneous bone formation model [43]. Further evaluation of the direct effects of SDF-1α on MSC performance with respect to proliferation and (trans)differentiation, as has been suggested by other studies [41,42,44,45], could explain some of the results.

Conclusions

In summary, we demonstrated for the first time that SDF-1α incorporated in a hybrid hydrogel-based construct is effective in stimulating seeded goat EPCs in vitro and that this cell/chemokine therapy induces vessel formation in vivo. In addition, SDF-1α could replace seeded EPCs resulting in elaborate interconnected vessel networks, while not affecting bone onset, bone volumes, or bone contact percentages. Altogether, these results hold promise for the design of cell/chemokine-based vascular bone grafts on the larger scale.

Acknowledgments

This research forms part of the Project P2.04 BONE-IP of the research program of the BioMedical Materials Institute, cofunded by the Dutch Ministry of Economic Affairs, Agriculture and Innovation. The authors acknowledge financial support by the Anna Foundation for Scientific Research to R.E. (Anna Fonds; grant number: O.2011/23).

Author Disclosure Statement

No competing financial interests exist.

References

1. Hausman MR, MB Schaffler and RJ Majeska. (2001). Prevention of fracture healing in rats by an inhibitor of angiogenesis. Bone 29:560–564.
2. Carano RA and EH Filvaroff. (2003). Angiogenesis and bone repair. Drug Discov Today 8:980–989.
3. Griffith CK, C Miller, RC Sainson, JW Calvert, NL Jeon, CC Hughes and SC George. (2005). Diffusion limits of an in vitro thick prevascularized tissue. Tissue Eng 11:257–266.
4. Hsiong SX and DJ Mooney. (2006). Regeneration of vascularized bone. Periodontol 2000 41:109–122.
5. Zhou J, H Lin, T Fang, X Li, W Dai, T Uemura and J Dong. (2010). The repair of large segmental bone defects in the rabbit with vascularized tissue engineered bone. Biomaterials 31:1171–1179.
6. Seebach C, D Henrich, C Kahling, K Wilhelm, AE Tami, M Alini and I Marzi. (2010). Endothelial progenitor cells and mesenchymal stem cells seeded onto beta-TCP granules enhance early vascularization and bone healing in a critical-sized bone defect in rats. Tissue Eng Part A 16:1961–1970.
7. Fedorovich NE, RT Haverslag, WJ Dhert and J Alblas. (2010). The role of endothelial progenitor cells in prevascularized bone tissue engineering: development of heterogeneous constructs. Tissue Eng Part A 16:2355–2367.
8. Usami K, H Mizuno, K Okada, Y Narita, M Aoki, T Kondo, D Mizuno, J Mase, H Nishiguchi, H Kagami and M Ueda. (2009). Composite implantation of mesenchymal stem cells with endothelial progenitor cells enhances tissue-engineered bone formation. J Biomed Mater Res A 90:730–741.
9. Liu Y, SH Teoh, MS Chong, ES Lee, CN Mattar, NK Randhawa, ZY Zhang, RJ Medina, RD Kamm, et al. (2012). Vasculogenic and osteogenesis-enhancing potential of human umbilical cord blood endothelial colony-forming cells. Stem Cells 30:1911–1924.
10. Kaigler D, PH Krebsbach, ER West, K Horger, YC Huang and DJ Mooney. (2005). Endothelial cell modulation of bone marrow stromal cell osteogenic potential. FASEB J 19:665–667.
11. Wenger A, A Stahl, H Weber, G Finkenzeller, HG Augustin, GB Stark and U Kneser. (2004). Modulation of in vitro angiogenesis in a three-dimensional spheroidal coculture model for bone tissue engineering. Tissue Eng 10:1536–1547.
12. Rao RR, AW Peterson, J Ceccarelli, AJ Putnam and JP Stegemann. (2012). Matrix composition regulates three-dimensional network formation by endothelial cells and mesenchymal stem cells in collagen/fibrin materials. Angiogenesis 15:253–264.
13. Santos MI, RE Unger, RA Sousa, RL Reis and CJ Kirkpatrick. (2009). Crosstalk between osteoblasts and endothelial cells co-cultured on a polycaprolactone-starch scaffold and the in vitro development of vascularization. Biomaterials 30:4407–4415.
14. Melero-Martin JM, ZA Khan, A Picard, X Wu, S Paruchuri and J Bischoff. (2007). In vivo vasculogenic potential of human blood-derived endothelial progenitor cells. Blood 109:4761–4768.
15. Kaigler D, PH Krebsbach, Z Wang, ER West, K Horger and DJ Mooney. (2006). Transplanted endothelial cells enhance orthotopic bone regeneration. J Dent Res 85:633–637.
16. Lee KY, MC Peters, KW Anderson and DJ Mooney. (2000). Controlled growth factor release from synthetic extracellular matrices. Nature 408:998–1000.
17. Kaigler D, PH Krebsbach, PJ Polverini and DJ Mooney. (2003). Role of vascular endothelial growth factor in bone marrow stromal cell modulation of endothelial cells. Tissue Eng 9:95–103.
18. Kempen DH, L Lu, A Heijink, TE Hefferan, LB Creemers, A Maran, MJ Yaszemski and WJ Dhert. (2009). Effect of local sequential VEGF and BMP-2 delivery on ectopic and orthotopic bone regeneration. Biomaterials 30:2816–2825.
19. Street J, M Bao, L deGuzman, S Bunting, FV Peale, Jr., N Ferrara, H Steinmetz, J Hoeffel, JL Cleland, et al. (2002). Vascular endothelial growth factor stimulates bone repair by promoting angiogenesis and bone turnover. Proc Natl Acad Sci U S A 99:9656–9661.
20. Mirshahi F, J Pourtau, H Li, M Muraine, V Trochon, E Legrand, J Vannier, J Soria, M Vasse and C Soria. (2000). SDF-1 activity on microvascular endothelial cells: consequences on angiogenesis in in vitro and in vivo models. Thromb Res 99:587–594.
21. Chen T, H Bai, Y Shao, M Arzigian, V Janzen, E Attar, Y Xie, DT Scadden and ZZ Wang. (2007). Stromal cell-derived factor-1/CXCR4 signaling modifies the capillary-like organization of human embryonic stem cell-derived endothelium in vitro. Stem Cells 25:392–401.
22. Kuraitis D, P Zhang, Y Zhang, DT Padavan, K McEwan, T Sofrenovic, D McKee, J Zhang, M Griffith, et al. (2011). A stromal cell-derived factor-1 releasing matrix enhances the progenitor cell response and blood vessel growth in ischaemic skeletal muscle. Eur Cell Mater 22:109–123.

23. Thevenot PT, AM Nair, J Shen, P Lotfi, CY Ko and L Tang. (2010). The effect of incorporation of SDF-1alpha into PLGA scaffolds on stem cell recruitment and the inflammatory response. Biomaterials 31:3997–4008.
24. Kitaori T, H Ito, EM Schwarz, R Tsutsumi, H Yoshitomi, S Oishi, M Nakano, N Fujii, T Nagasawa and T Nakamura. (2009). Stromal cell-derived factor 1/CXCR4 signaling is critical for the recruitment of mesenchymal stem cells to the fracture site during skeletal repair in a mouse model. Arthritis Rheum 60:813–823.
25. Liu X, S Zhou, Y Li and J Yan. (2012). Stromal cell derived factor-1alpha enhances bone formation based on in situ recruitment: a histologic and histometric study in rabbit calvaria. Biotechnol Lett 34:387–395.
26. Kucia M, R Reca, K Miekus, J Wanzeck, W Wojakowski, A Janowska-Wieczorek, J Ratajczak and MZ Ratajczak. (2005). Trafficking of normal stem cells and metastasis of cancer stem cells involve similar mechanisms: pivotal role of the SDF-1-CXCR4 axis. Stem Cells 23:879–894.
27. Kimura Y and Y Tabata. (2010). Controlled release of stromal-cell-derived factor-1 from gelatin hydrogels enhances angiogenesis. J Biomater Sci Polym Ed 21:37–51.
28. Urist MR, O Nilsson, J Rasmussen, W Hirota, T Lovell, T Schmalzreid and GA Finerman. (1987). Bone regeneration under the influence of a bone morphogenetic protein (BMP) beta tricalcium phosphate (TCP) composite in skull trephine defects in dogs. Clin Orthop Relat Res 214:295–304.
29. Wang EA, V Rosen, JS D'Alessandro, M Bauduy, P Cordes, T Harada, DI Israel, RM Hewick, KM Kerns, P LaPan, et al. (1990). Recombinant human bone morphogenetic protein induces bone formation. Proc Natl Acad Sci U S A 87:2220–2224.
30. Lissenberg-Thunnissen SN, DJ de Gorter, CF Sier and IB Schipper. (2011). Use and efficacy of bone morphogenetic proteins in fracture healing. Int Orthop 35:1271–1280.
31. Geuze RE, MC Kruyt, AJ Verbout, J Alblas and WJ Dhert. (2008). Comparing various off-the-shelf methods for bone tissue engineering in a large-animal ectopic implantation model: bone marrow, allogeneic bone marrow stromal cells, and platelet gel. Tissue Eng Part A 14:1435–1443.
32. Geuze RE, PA Everts, MC Kruyt, AJ Verbout, J Alblas and WJ Dhert. (2009). Orthotopic location has limited benefit from allogeneic or autologous multipotent stromal cells seeded on ceramic scaffolds. Tissue Eng Part A 15:3231–3239.
33. Kruyt MC, JD de Bruijn, H Yuan, CA van Blitterswijk, AJ Verbout, FC Oner and WJ Dhert. (2004). Optimization of bone tissue engineering in goats: a peroperative seeding method using cryopreserved cells and localized bone formation in calcium phosphate scaffolds. Transplantation 77:359–365.
34. Lesman A, J Koffler, R Atlas, YJ Blinder, Z Kam and S Levenberg. (2011). Engineering vessel-like networks within multicellular fibrin-based constructs. Biomaterials 32:7856–7869.
35. Niemisto A, V Dunmire, O Yli-Harja, W Zhang and I Shmulevich. (2005). Robust quantification of in vitro angiogenesis through image analysis. IEEE Trans Med Imaging 24:549–553.
36. Yoon CH, J Hur, KW Park, JH Kim, CS Lee, IY Oh, TY Kim, HJ Cho, HJ Kang, et al. (2005). Synergistic neovascularization by mixed transplantation of early endothelial progenitor cells and late outgrowth endothelial cells: the role of angiogenic cytokines and matrix metalloproteinases. Circulation 112:1618–1627.
37. Rae PC, RD Kelly, S Egginton and JC St John. (2011). Angiogenic potential of endothelial progenitor cells and embryonic stem cells. Vasc Cell 3:11.
38. Hur J, CH Yoon, HS Kim, JH Choi, HJ Kang, KK Hwang, BH Oh, MM Lee and YB Park. (2004). Characterization of two types of endothelial progenitor cells and their different contributions to neovasculogenesis. Arterioscler Thromb Vasc Biol 24:288–293.
39. Lin RZ and JM Melero-Martin. (2011). Bioengineering human microvascular networks in immunodeficient mice. J Vis Exp 53:e3065.
40. Au P, LM Daheron, DG Duda, KS Cohen, JA Tyrrell, RM Lanning, D Fukumura, DT Scadden and RK Jain. (2008). Differential in vivo potential of endothelial progenitor cells from human umbilical cord blood and adult peripheral blood to form functional long-lasting vessels. Blood 111:1302–1305.
41. Wang CH, TM Wang, TH Young, YK Lai and ML Yen. (2013). The critical role of ECM proteins within the human MSC niche in endothelial differentiation. Biomaterials 34:4223–4234.
42. Janeczek Portalska K, A Leferink, N Groen, H Fernandes, L Moroni, C van Blitterswijk and J de Boer. (2012). Endothelial differentiation of mesenchymal stromal cells. PLoS One 7:e46842.
43. Eman RM, FC Oner, MMP Kruyt, W Dhert and J Alblas. (2014). Stromal cell-derived factor-1 stimulates cell recruitment, vascularization and osteogenic differentiation. Tissue Eng Part A 20:466–473.
44. Kortesidis A, A Zannettino, S Isenmann, S Shi, T Lapidot and S Gronthos. (2005). Stromal-derived factor-1 promotes the growth, survival, and development of human bone marrow stromal stem cells. Blood 105:3793–3801.
45. Du L, P Yang and S Ge. (2012). Stromal cell-derived factor-1 significantly induces proliferation, migration, and collagen type I expression in a human periodontal ligament stem cell subpopulation. J Periodontol 83:379–388.

Address correspondence to:
Jacqueline Alblas, PhD
Department of Orthopedics
University Medical Center Utrecht, Rm G05.228
P.O. Box 85500
Utrecht 3508 GA
The Netherlands

E-mail: j.alblas@umcutrecht.nl

Received for publication November 15, 2013
Accepted after revision July 15, 2014
Prepublished on Liebert Instant Online July 18, 2014